

# *The effects of chloride ion and organic extractants on electrowon zinc deposits*

D. J. MACKINNON, J. M. BRANNEN, V. I. LAKSHMANAN\*

*Metallurgical Chemistry Section, Mineral Sciences Laboratories, CANMET, Department of Energy, Mines and Resources, Ottawa, K1A 0G1, Canada*

Received 16 May 1979

The effects of chloride ion and the organic extractants: Kelex 100, Versatic 911, di-2-ethylhexyl phosphoric acid, tri-*n*-butyl phosphate, LIX65N and Alamine 336 on the structure of 1 h zinc deposits electrowon from synthetic and industrial acid sulphate electrolytes are presented. Under simulated tankhouse conditions the effect of chloride ion concentration on the zinc deposit morphology and orientation becomes significant only at the 500 mg l<sup>-1</sup> level. The tolerance limit of the zinc deposits to organic extractants such as Kelex 100 is extremely low. In some cases the adverse effect of these organic impurities is offset by the presence of chloride ion in the electrolyte. Purification of electrolyte contaminated with organic extractants by activated charcoal results in a vastly improved zinc deposit structure. Organic extractants such as Kelex 100 and TBP which have an adverse effect on the zinc deposits, also have a pronounced effect on the zinc deposition polarization curve.

## 1. Introduction

Chemical leaching using aqueous chloride solutions (FeCl<sub>3</sub>, HCl, CuCl<sub>2</sub>) [1–3] and dry chlorination (Cl<sub>2</sub>) [4] are some of the methods currently under investigation for the treatment of Zn–Pb–Cu–Fe sulphide ores. These methods eventually result in chloride leach liquors containing various metallic elements. Recent work has shown that the separation of zinc from chloride leach liquors by solvent extraction is feasible even at high chloride ion concentrations [5, 6]. In addition to producing a pure concentrated solution of zinc chloride, which may conceivably be used to electrowin Zn metal and produce Cl<sub>2</sub> gas for recycling, the solvent extraction technique also offers the option of converting the chloride electrolyte to the sulphate system from which zinc could be recovered by conventional electrolysis; in this case HCl would be a by-product for possible recycling to a leaching stage [7, 8]. The treatment of chloride solutions by solvent extraction processes to produce sulphate tankhouse liquors could result in the

presence of chloride ion and organic extractant in the electrowinning stage. A similar situation could arise by treating high copper-containing conventional zinc sulphate electrolytes, produced by a regular or Sheritt-Gordon-type pressure leach process, by solvent extraction methods to recover the copper; in the process of separating the copper, the zinc sulphate electrolyte may become contaminated with solvent extraction reagents. Furthermore, a high chloride ion-containing zinc sulphate electrolyte could also be realized because processes such as oxygen pressure leaching or sulphation roasting lack the inherently good chloride volatilization of conventional dead roasting. If a combined solvent extraction–electrowinning process for zinc recovery is to become a viable commercial operation, then information on the tolerance limits of chloride ion and/or dissolved or entrained organic extractants on the electrodeposition of zinc will be required.

Fukubayashi *et al.* [9] briefly studied the effect of HCl as an impurity addition to zinc sulphate electrolyte. They observed an (002) basal plane oriented zinc deposit for HCl additions from 100 to 2000 mg l<sup>-1</sup>. The cell voltage increased and the current efficiency decreased with increased

\* Present address: Research and Development Division, Eldorado Nuclear Ltd, 400–255 Albert Street, Ottawa, Canada K1P 6A9.

additions of HCl. Fosnacht and O'Keefe [10] later reported that chloride ion, in the absence of glue and other impurities, had little effect on the current efficiency or zinc deposit morphology.

With respect to organic additives and/or impurities, only the effect of glue on the zinc deposit structure has been studied in any detail [11]. It is well established that small additions of glue (15 to 30 mg l<sup>-1</sup>) smooth the zinc deposit by refining the grain size and that certain combinations of glue and inorganic additives, e.g. glue + antimony [12], result in the optimization of the current efficiency. It is also well established [12] that the current efficiency decreases with increasing glue additions to the electrolyte. Fosnacht and O'Keefe [10] have observed, however, that the presence of chloride ion reduces the glue effect on the current efficiency such that the amount of 'active' glue in the electrolyte has decreased.

Organic extractants which are currently being evaluated for separating zinc from chloride liquors or for producing purified, concentrated zinc chloride solutions include Kelex 100, Versatic 911, tri-*n*-butyl phosphate (TBP), di-2 ethylhexyl phosphoric acid (D2EHPA) and Alamine 336. LIX65N, an extractant used for Cu, has also been included in this study since the situation may arise in which a copper-containing zinc sulphate electrolyte may be processed for Cu recovery by solvent extraction techniques prior to zinc electrolysis. The results of a systematic investigation on the effects of chloride ion, organic extractants and various combinations of chloride ion and organic extractant on the morphology and orientation of 1 h zinc deposits are reported.

## 2. Experimental

### 2.1. Materials and apparatus

The electrolyte was prepared from reagent grade ZnSO<sub>4</sub> · 7H<sub>2</sub>O and ultrapure sulphuric acid. The electrolysis solution contained 55 g l<sup>-1</sup> Zn and 150 g l<sup>-1</sup> H<sub>2</sub>SO<sub>4</sub>. The electrolyte was pre-treated with SrCO<sub>3</sub>, and Pt anodes were used during electrolysis in order to minimize lead contamination of the zinc deposits [13]. Chloride ion (as NaCl) and the various organic extractants were added as aliquots from their respective stock solutions. The electrolysis cell and electrode assembly have been

described previously [14]. The anodes were cut from 0.1 cm thick Pt sheet and measured 15.2 × 2.5 cm, although for certain tests 0.75 wt% Ag-Pb anodes were also used. The aluminium cathode (15.2 × 3.2 × 0.32 cm thick) was fabricated from commercial grade aluminium (obtained from Cominco) and was mounted in the cell so that the total deposit area was 10.2 cm<sup>2</sup>.

### 2.2. Electrolyte purification

Electrolytes containing dissolved organic extractants in concentrations in excess of their solubility limits (Kelex 100, 10 mg l<sup>-1</sup>; Versatic 911, 300 mg l<sup>-1</sup>, D2EHPA, TBP and Alamine 336, 25 mg l<sup>-1</sup>) and Cl<sup>-</sup> to 500 mg l<sup>-1</sup>, alone and in various combinations, were treated with activated carbon as follows: 1 l of electrolyte containing the organic extractant(s) was heated to 60°C; 5 g activated carbon was added and the mixture was stirred for 30 min at 60°C. The mixture was then filtered to remove the activated carbon. In some cases this procedure was repeated a second time using a fresh batch of activated carbon.

### 2.3. Electrolysis

Operating conditions of 75 A ft<sup>-2</sup> (807 A m<sup>-2</sup>), electrolysis time of 1 h and 35°C were used for most of the experiments although additional tests were conducted at 25 A ft<sup>-2</sup> (269 A m<sup>-2</sup>). The variables studied were the concentrations of chloride ion, Kelex 100, Versatic 911, D2EHPA, TBP, LIX65N and Alamine 336.

### 2.4. Deposit examination

Sections of the deposits were examined by X-ray diffraction (XRD) to determine their preferred orientation relative to the ASTM standard for zinc powder, by scanning electron microscopy (SEM) to determine their surface morphology and by optical microscopy (OM) to study their cross-sections.

### 2.5. Polarization studies

Potentiodynamic *i*-*V* curves were obtained at a linear potential scan rate of 1 mV s<sup>-1</sup> to determine the polarization characteristics of zinc deposition

in the presence of chloride ion and/or organic extractants.

### 3. Results and discussion

#### 3.1. The effect of chloride ion

**3.1.1. Pt anodes.** Chloride ion at  $100 \text{ mg l}^{-1}$  had no significant effect on zinc deposit morphology or crystallographic orientation (Table 1) obtained at  $269 \text{ A m}^{-2}$  as compared to addition-free acid sulphate electrolyte. At  $500 \text{ mg l}^{-1}$  chloride ion concentration, the (1 1 2) preferred orientation observed at lower concentrations changed to a (1 1 2) (1 0 5) preferred orientation with no observable change in morphology.

The deposit morphology obtained at  $807 \text{ A m}^{-2}$  from an electrolyte containing  $500 \text{ mg l}^{-1} \text{ Cl}^{-}$  is shown in the SEM photomicrograph, Fig. 1a. In this case the basal platelets are aligned at low angles to the Al substrate. The preferred orientation changes from (1 1 2) to (1 0 3) (1 1 4) with increasing chloride ion concentration (Table 1). The cross-sections of the deposits are all relatively smooth and even, indicating that  $\text{Cl}^{-}$  concentration up to  $500 \text{ mg l}^{-1}$  has no harmful effect on the deposit growth (Fig. 1b).

**3.1.2. 0.75 wt% Ag–Pb anodes.** The effect of chloride ion on the zinc deposit structure was also

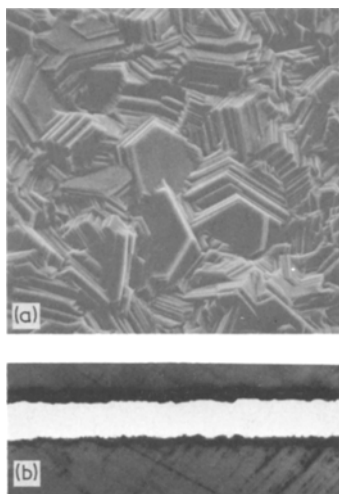


Fig. 1. (a) SEM photomicrograph and (b) OM photomicrograph showing the effect of  $500 \text{ mg l}^{-1}$  chloride ion on the zinc deposit morphology and cross-section, at  $807 \text{ A m}^{-2}$ . (a)  $\times 840$ ; (b)  $\times 120$ .

studied using 0.75 wt% Ag–Pb anodes which are commonly used in commercial zinc electrowinning. The resulting deposit morphologies were characteristic of lead contamination of the zinc deposits [13]. The deposit orientations and lead assays (Table 1) confirmed this. The lead contamination apparently originated from corrosion of the Ag–Pb anodes.

#### 3.2. Effect of organic extractants

**3.2.1. Kelex 100, Versatic 911, chloride ion and antimony.** The commercial extractants, Kelex 100 and Versatic 911 are capable of extracting zinc from both sulphate and chloride media; moreover, a combination of Kelex 100 and Versatic 911 leads to synergistic enhancement of zinc extraction [6]. Thus the effects of Kelex 100 and Versatic 911, both individually and in combination, on the zinc deposit morphology and orientation were assessed. Because both chloride ion [10] and antimony additions [12, 14] to zinc sulphate electrolyte are known to counteract or optimize the effect of glue on the current efficiency and zinc deposit structure, their effect in the presence of these organic extractants was also examined.

The effect of Kelex and Kelex +  $\text{Cl}^{-}$  on the morphology of the zinc deposits is indicated in the SEM photomicrographs shown in Fig. 2, and in Table 2. Kelex 100 at  $1 \text{ mg l}^{-1}$  gave a (1 0 1) orientation at  $269 \text{ A m}^{-2}$  and a (1 0 3) orientation with deep circular pits in the zinc deposits (Fig. 2a and c) at  $807 \text{ A m}^{-2}$ . The addition of  $\text{Cl}^{-} \geq 10 \text{ mg l}^{-1}$  counteracted the effect of Kelex 100 on the zinc deposits, giving smooth, compact deposits with a (1 1 2) orientation (Fig. 2b and d). The addition of  $\text{Cl}^{-}$  was not effective in counteracting the effect of  $> 2 \text{ mg l}^{-1}$  Kelex 100 on the zinc deposits. At Kelex 100 concentrations  $> 2 \text{ mg l}^{-1}$ , the zinc deposits exhibited severe 'organic burn' which was manifested as a black powder.

Antimony additions to electrolyte containing Kelex 100 counteracted the effect of Kelex 100 on the zinc deposits (Table 2). At higher Sb concentrations ( $0.08 \text{ mg l}^{-1}$ ), the zinc deposit exhibited some re-solution.

Versatic 911 additions to zinc electrolyte changed the zinc deposit orientation from (1 1 2)  $\rightarrow$  (1 1 4)  $\rightarrow$  (1 0 2)  $\rightarrow$  (1 0 1) with increasing concentrations (Table 3). The zinc deposits

Table 1. The effect of  $\text{Cl}^-$  on the preferred orientation of zinc deposits obtained from acid sulphate electrolyte. Electrolysis conditions:  $55 \text{ g l}^{-1} \text{ Zn}$ ,  $150 \text{ g l}^{-1} \text{ H}_2\text{SO}_4$ ,  $35^\circ \text{ C}$

$\text{Cl}^-$ ( $\text{mg l}^{-1}$ )	Crystallographic orientation	Lead content of Zn deposits (%)	Corresponding figure in text
<i>at 269 A m<sup>-2</sup>; Pt anodes</i>			
0	(1 1 2) (1 1 4) (1 0 2)	—	—
10	(1 1 2)	—	—
50	(1 1 2)	—	—
100	(1 1 2)	—	—
500	(1 1 2) (1 0 5)	—	—
<i>at 807 A m<sup>-2</sup>; Pt anodes</i>			
0	(1 1 2) (1 1 4) (1 0 2)	—	—
10	(1 1 2)	—	—
50	(1 0 3) (1 0 4)	—	—
100	(1 1 4) (1 0 3)	—	—
500	(1 0 3) (1 0 5)	—	1a, b
<i>at 807 A m<sup>-2</sup>; Pb-Ag anodes</i>			
0	(1 0 1) (1 0 2)	0.008	—
10	(1 0 1) (1 0 2)	0.008	—
50	(1 0 1)	0.003	—
100	(1 0 1) (1 0 2)	0.004	—
500	(1 0 1) (1 0 2)	0.016	—

\* Relative to ASTM standard for Zn powder.

showed increasingly nodular growth and finer grain size with increasing Versatic 911 and  $\text{Cl}^-$  additions (Fig. 3).

The combined effects of  $1 \text{ mg l}^{-1}$  Kelex 100,  $50 \text{ mg l}^{-1}$  Versatic 911 and  $500 \text{ mg l}^{-1} \text{ Cl}^-$  resulted in a powdery, poorly crystalline zinc deposit as indicated in the SEM photomicrograph (Fig. 3d).

This deposit was not suitable for crystallographic orientation analysis.

3.2.2. *Di-2-ethylhexyl phosphoric acid (D2EHPA), Tri-n-butyl phosphate (TBP), Alamine 336, LIX65N, chloride ion and antimony.* Other extractants such as D2EHPA, TBP and Alamine

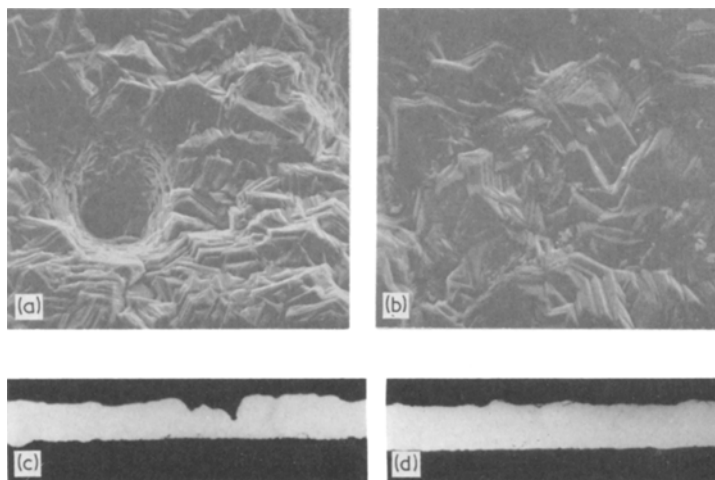


Fig. 2. (a, b) SEM photomicrographs and (c, d) OM photomicrographs showing the effects of Kelex 100 and Kelex 100 +  $\text{Cl}^-$  on the morphology and cross-sections of zinc deposits. (a)  $1 \text{ mg l}^{-1}$  Kelex 100 ( $\times 840$ ); (b)  $1 \text{ mg l}^{-1}$  Kelex 100,  $500 \text{ mg l}^{-1} \text{ Cl}^-$  ( $\times 840$ ); (c)  $1 \text{ mg l}^{-1}$  Kelex 100 ( $\times 120$ ); (d)  $1 \text{ mg l}^{-1}$  Kelex 100,  $500 \text{ mg l}^{-1} \text{ Cl}^-$  ( $\times 120$ ); all at  $807 \text{ A m}^{-2}$ .

Table 2. The effect of Kelex 100,  $Cl^-$  and Sb concentrations on the preferred orientation of zinc deposits obtained from acid sulphate electrolyte. Electrolysis conditions:  $55\text{ g l}^{-1}\text{ Zn}$ ,  $150\text{ g l}^{-1}\text{ H}_2\text{SO}_4$ ,  $807\text{ A m}^{-2}$ ,  $35^\circ\text{ C}$

Kelex 100 ( $\text{mg l}^{-1}$ )	$Cl^-$ ( $\text{mg l}^{-1}$ )	Sb ( $\text{mg l}^{-1}$ )	Orientation*	Corresponding figure in text
0	—	—	(1 1 2)	—
0.2	—	—	(1 0 1) (1 0 2)	—
0.6	—	—	(1 0 1)	—
1.0	—	—	(1 0 3)	2a, c
1.0	10	—	(1 0 3)	—
1.0	50	—	(1 1 2) (1 0 1)	—
1.0	100	—	(1 1 2)	—
1.0	500	—	(1 1 2)	2b, d
1.0	—	0.04	(1 1 2)	—
1.0	—	0.08	(1 1 0)	—
1.0	50	0.04	(1 1 2)	—
1.0	50	0.08	(1 1 2) (1 1 0)	—
1.0	500	0.08	(1 0 1)	—

\* Relative to ASTM standard for zinc powder.

336 have also been used to extract zinc from both sulphate and chloride media [5, 7, 8]. Alamine 336 extracts zinc from chloride solutions as a zinc-chloro complex anion; if conversion to a zinc sulphate electrolyte is required, then the zinc must be re-extracted from the purified zinc solution using a cation exchanger such as D2EHPA. Thus, it is possible to have both D2EHPA and Alamine carried over into the zinc sulphate electrolyte.

Therefore, in addition to studying the effects of the individual extractants, D2EHPA, TBP, and Alamine 336, on the zinc deposit structure, the effects of various combinations of these organics were also studied. The effect of LIX65N on the zinc deposit structure was briefly studied for the reason mentioned earlier.

The addition of D2EHPA to zinc electrolyte gave zinc deposits with relatively large hexagonal

Table 3. The effect of Versatic 911,  $Cl^-$  and Sb concentrations on the preferred orientation of zinc deposits obtained from acid sulphate electrolyte. Electrolysis conditions:  $55\text{ g l}^{-1}\text{ Zn}$ ,  $150\text{ g l}^{-1}\text{ H}_2\text{SO}_4$ ,  $807\text{ A m}^{-2}$ ,  $35^\circ\text{ C}$

Versatic 911 ( $\text{mg l}^{-1}$ )	$Cl^-$ ( $\text{mg l}^{-1}$ )	Sb ( $\text{mg l}^{-1}$ )	Orientation*	Corresponding figure in text
0	0	0	(1 1 2)	—
5	—	—	(1 1 4) (1 0 3)	3a, e
10	—	—	(1 0 3) (1 0 2)	—
25	—	—	(1 0 2) (1 0 3)	—
50	—	—	(1 0 1)	3b, f
100	—	—	(1 0 1)	—
50	10	—	(1 0 1)	—
50	50	—	(1 0 1)	—
50	100	—	(1 0 1)	—
50	500	—	(1 0 1)	3c, g
50	—	0.04	(1 0 1)	—
50	—	0.08	(1 0 1)	—
50	500	0.04	(1 0 1)	—
50	500	0.08	(1 1 4)	—

\* Relative to ASTM standard for Zn powder.

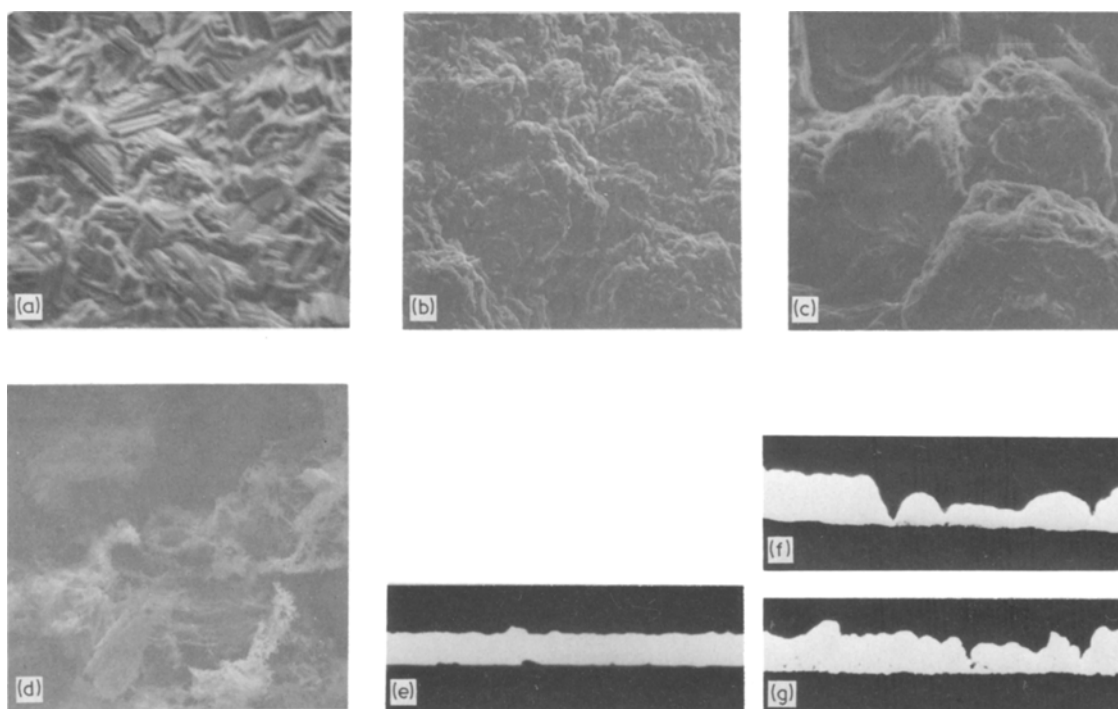


Fig. 3. (a–d) SEM photomicrographs and (e–g) OM photomicrographs showing the effect of Versatic 911, Versatic 911 +  $\text{Cl}^-$  and Versatic 911 + Kelex 100 +  $\text{Cl}^-$  on the morphology and cross-sections of zinc deposits at  $807 \text{ A m}^{-2}$ . (a)  $5 \text{ mg l}^{-1}$  Versatic 911 ( $\times 840$ ); (b)  $50 \text{ mg l}^{-1}$  Versatic 911 ( $\times 840$ ); (c)  $50 \text{ mg l}^{-1}$  Versatic 911,  $500 \text{ mg l}^{-1} \text{ Cl}^-$  ( $\times 840$ ); (d)  $50 \text{ mg l}^{-1}$  Versatic 911,  $1 \text{ mg l}^{-1}$  Kelex 100,  $500 \text{ mg l}^{-1} \text{ Cl}^-$  ( $\times 840$ ); (e)  $5 \text{ mg l}^{-1}$  Versatic 911 ( $\times 120$ ); (f)  $50 \text{ mg l}^{-1}$  Versatic 911 ( $\times 120$ ); (g)  $50 \text{ mg l}^{-1}$  Versatic 911,  $500 \text{ mg l}^{-1} \text{ Cl}^-$  ( $\times 120$ ).

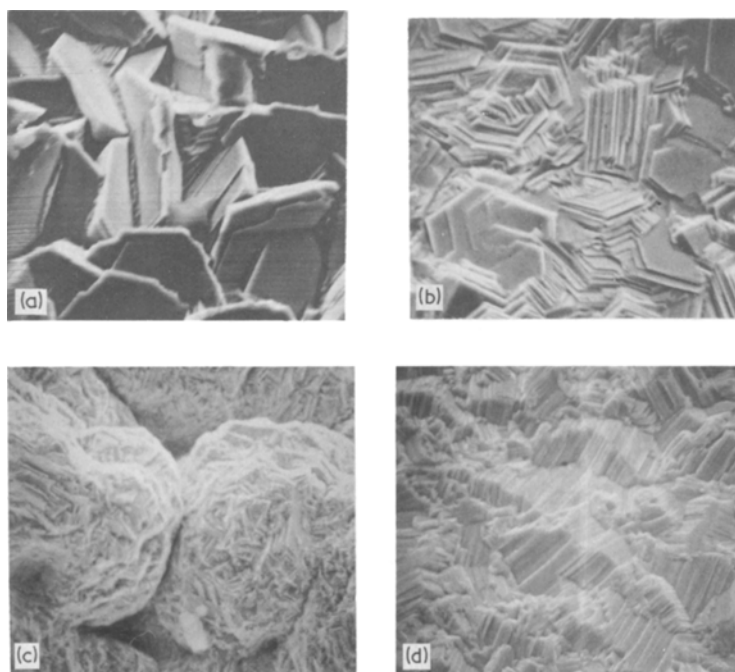


Fig. 4. SEM photomicrographs showing the effect of D2EHPA, D2EHPA +  $\text{Cl}^-$ , D2EHPA + Sb and D2EHPA +  $\text{Cl}^-$  + Sb on the morphology of zinc deposits obtained at  $807 \text{ A m}^{-2}$ . (a)  $5 \text{ mg l}^{-1}$  D2EHPA ( $\times 840$ ); (b)  $5 \text{ mg l}^{-1}$  D2EHPA,  $100 \text{ mg l}^{-1} \text{ Cl}^-$  ( $\times 840$ ); (c)  $5 \text{ mg l}^{-1}$  D2EHPA,  $0.04 \text{ mg l}^{-1} \text{ Sb}$  ( $\times 840$ ); (d)  $5 \text{ mg l}^{-1}$  D2EHPA,  $0.08 \text{ mg l}^{-1} \text{ Sb}$ ,  $100 \text{ mg l}^{-1} \text{ Cl}^-$  ( $\times 840$ ).

Table 4. The effect of D2EHPA,  $Cl^-$  and Sb concentrations on the preferred orientation of zinc deposits obtained from acid sulphate electrolyte. Electrolysis conditions:  $55\text{ g l}^{-1}$  Zn,  $150\text{ g l}^{-1}$   $H_2SO_4$ ,  $807\text{ A m}^{-2}$ ,  $35^\circ\text{ C}$

D2EHPA ( $\text{mg l}^{-1}$ )	$Cl^-$ ( $\text{mg l}^{-1}$ )	Sb ( $\text{mg l}^{-1}$ )	Orientation*	Corresponding figure in text
0	0	0	(1 1 2)	—
3	—	—	(1 0 3) (0 0 2)	—
5	—	—	(1 0 2) (1 0 1)	4a
10	—	—	(1 0 1)	—
5	10	—	(0 0 2)	—
5	50	—	(0 0 2)	—
5	100	—	(0 0 2)	4b
3	500	—	(0 0 2)	—
5	—	0.04	(1 0 1)	4c
5	—	0.08	(1 0 1)	—
5	100	0.04	(1 0 3) (1 0 2)	—
5	100	0.08	(1 1 2) (1 1 0)	4d
5	500	0.08	(1 1 2)	—

\* Relative to ASTM standard for Zn powder.

crystals (Fig. 4a) with a preferred orientation of (1 0 1) (1 0 2), Table 4. The combined additions of D2EHPA and  $Cl^-$  gave hexagonal basal platelets (Fig. 4b), with preferred orientations of (0 0 2). The combined additions of D2EHPA and Sb gave zinc deposit structures consisting of large spherical nodules with voids occurring at grain boundaries (Fig. 4c) and a predominant orientation of (1 0 1). The combined additions of D2EHPA,  $Cl^-$  and Sb gave more vertically oriented zinc deposit structures with preferred orientations of (1 1 2) (1 1 0) (Fig. 4d).

Both TBP and Alamine 336 additions, alone

or in combination with  $Cl^-$  and Sb, had similar effects on the zinc deposit morphology and orientation as those observed with D2EHPA (Tables 5 and 6).

The presence of both D2EHPA and Alamine 336 in the electrolyte ( $10\text{ mg l}^{-1}$  each) resulted in zinc deposits which had a predominant (1 0 1) orientation. The SEM photomicrographs revealed that the deposits consisted of well-defined hexagonal platelets aligned at intermediate angles to the aluminium cathode, similar to that depicted in Fig. 4a. Although the deposit morphology and orientation remained essentially the same for

Table 5. The effect of TBP,  $Cl^-$  and Sb concentrations on the preferred orientation of zinc deposits obtained from acid sulphate electrolyte. Electrolysis conditions:  $55\text{ g l}^{-1}$  Zn,  $150\text{ g l}^{-1}$   $H_2SO_4$ ,  $807\text{ A m}^{-2}$ ,  $35^\circ\text{ C}$

TBP ( $\text{mg l}^{-1}$ )	$Cl^-$ ( $\text{mg l}^{-1}$ )	Sb ( $\text{mg l}^{-1}$ )	Orientation*
0	0	0	(1 1 2)
3	—	—	(1 1 4)
5	—	—	(1 0 2)
10	—	—	(1 0 2) (1 0 1)
10	10	—	(1 1 4)
10	50	—	(1 1 4) (1 1 2)
10	100	—	(1 1 4)
10	500	—	(0 0 2) (1 1 4)
5	500	—	(0 0 2)
5	—	0.08	(1 1 2) (1 1 4)
5	100	0.08	(1 1 2) (1 1 4)

\* Relative to ASTM standard for zinc powder.

Table 6. The effect of Alamine 336,  $\text{Cl}^-$  and Sb concentrations on the preferred orientation of zinc deposits obtained from acid sulphate electrolyte. Electrolysis conditions:  $55 \text{ g l}^{-1} \text{ Zn}$ ,  $150 \text{ g l}^{-1} \text{ H}_2\text{SO}_4$ ,  $807 \text{ A m}^{-2}$ ,  $35^\circ \text{ C}$

Alamine 336 ( $\text{mg l}^{-1}$ )	$\text{Cl}^-$ ( $\text{mg l}^{-1}$ )	Sb ( $\text{mg l}^{-1}$ )	Orientation*
0	0	0	(1 1 2)
3	—	—	(1 0 1) (1 1 2)
5	—	—	(1 1 2) (1 1 4)
10	—	—	(1 0 1) (1 1 4)
10	10	—	(1 0 1) (1 1 4)
10	50	—	(1 1 4) (1 0 1)
10	100	—	(1 0 1) (1 1 4)
10	500	—	(1 0 1)
5	500	—	(0 0 2)
5	—	0.08	(1 1 2) (1 0 1)
5	100	0.08	(1 1 2)

\* Relative to ASTM standard for zinc powder.

D2EHPA and Alamine 336 concentrations of  $10 \text{ mg l}^{-1}$  each, the zinc deposits obtained for these conditions showed signs of organic burn. The presence of various concentrations of  $\text{Cl}^-$  (to  $500 \text{ mg l}^{-1}$ ) did not alter the deposit morphology and orientation observed for D2EHPA and Alamine 336 without  $\text{Cl}^-$  additions.

The effect of LIX65N and LIX65N +  $\text{Cl}^-$  on the morphology and orientation of zinc deposits obtained from synthetic acid sulphate electrolyte was briefly examined. The presence of  $10 \text{ mg l}^{-1}$  LIX65N resulted in a zinc deposit morphology similar to that obtained in the presence of  $10 \text{ mg l}^{-1}$  TBP and having a (1 0 1) preferred orientation. Increasing amounts of LIX65N in the electrolyte, 50 and  $100 \text{ mg l}^{-1}$ , resulted in organic burn and the deposits obtained consisted of a mixture of black powder and metal. These deposits were not suitable for XRD or SEM analysis.

The addition of  $100 \text{ mg l}^{-1} \text{ Cl}^-$  to an electrolyte containing  $50 \text{ mg l}^{-1}$  LIX65N resulted in a metallic deposit (no organic burn observed) having a (1 0 1) preferred orientation.

### 3.3. Electrolyte purification with activated carbon

It is obvious from the data presented thus far that the zinc deposits have a very low tolerance limit for organic contaminants such as Kelex 100 and Versatic 911. This presents a serious problem

since these tolerance limits are considerably less than the solubility limits for these species in the electrolyte. Thus it becomes necessary to ensure that these contaminants are removed from the electrolyte prior to electrowinning the zinc. One method for doing this is to treat the electrolyte with activated carbon. Activated carbon treatment is widely used in the electroplating industry to remove oil, grease, addition agents and their decomposition products as well as other organic compounds [15].

The SEM photomicrographs in Fig. 5 compare the morphologies of deposits obtained from electrolytes purified with activated carbon with those obtained from untreated electrolyte under otherwise similar experimental conditions. Fig. 5a shows the deposit morphology obtained from an addition-free, activated carbon-treated electrolyte. This morphology type and the preferred deposit orientation (Table 7) were very similar to those obtained from the electrolyte which had not received the activated carbon treatment (Table 1).

The SEM photomicrographs, Figs. 5b and c, compare the morphologies of zinc deposits obtained from electrolytes containing  $10 \text{ mg l}^{-1}$  Kelex and  $300 \text{ mg l}^{-1}$  Versatic 911 with and without activated carbon purification, respectively. Fig. 5b indicates a powdery, dendritic deposit while Fig. 5c shows a deposit structure consisting of well-defined hexagonal platelets having a preferred basal, (0 0 2), orientation (Table 7).

The deposit obtained from an electrolyte containing  $25 \text{ mg l}^{-1}$  D2EHPA exhibited organic burn along its edges; the deposit morphology is shown in Fig. 5d which indicates large, poorly defined hexagonal platelets having an intermediate orientation (1 0 2) (1 1 4) (Table 7). The deposit obtained from a similar electrolyte purified by activated charcoal was crystalline and showed no evidence of organic burn. The SEM photomicrograph, Fig. 5e, shows the deposit to consist of well-defined hexagonal platelets. The orientation was (1 0 2) (1 0 3).

The deposit obtained from an electrolyte containing  $25 \text{ mg l}^{-1}$  TBP was black and powdery and hence not suitable for XRD or SEM. The presence of  $100 \text{ mg l}^{-1} \text{ Cl}^-$  in the electrolyte improved the deposit somewhat, resulting in a dark grey metallic product; however, the SEM revealed poorly defined platelets and large voids in the deposit



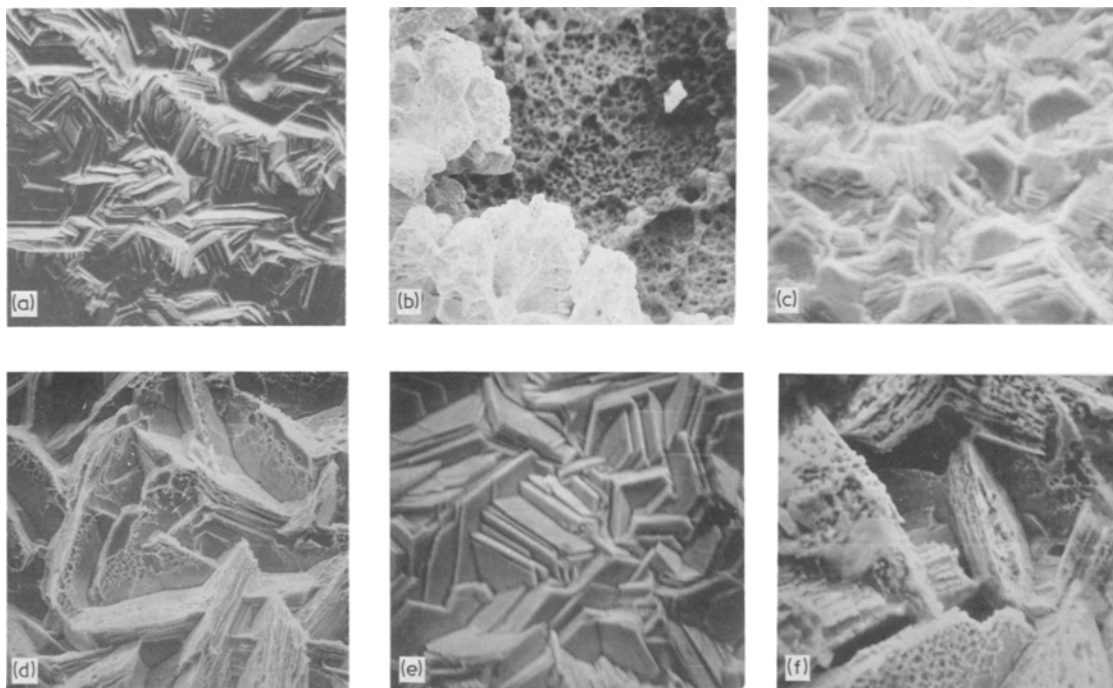


Fig. 5. SEM photomicrographs showing the effect of various organic extractants on the deposit morphology obtained from electrolyte treated with activated carbon at  $807 \text{ A m}^{-2}$ . (a) Addition-free, act. C treated ( $\times 840$ ); (b)  $10 \text{ mg l}^{-1}$  Kelex 100,  $300 \text{ mg l}^{-1}$  Versatic 911, no act. C ( $\times 840$ ); (c)  $10 \text{ mg l}^{-1}$  Kelex 100,  $300 \text{ mg l}^{-1}$  Versatic 911, act. C treated ( $\times 840$ ); (d)  $25 \text{ mg l}^{-1}$  D2EHPA, no act. C ( $\times 840$ ); (e)  $25 \text{ mg l}^{-1}$  D2EHPA, act. C treated; (f)  $25 \text{ mg l}^{-1}$  TBP,  $100 \text{ mg l}^{-1}$   $\text{Cl}^-$ , no act. C ( $\times 840$ ).

structure, Fig. 5f. Purification of the electrolyte containing  $25 \text{ mg l}^{-1}$  TBP with activated carbon resulted in a smooth deposit having an (002) orientation.

The presence of Alamine 336 ( $25 \text{ mg l}^{-1}$ ) or Alamine 336 and D2EHPA ( $10 \text{ mg l}^{-1}$  each) in the electrolyte gave zinc deposits which were composed of very large hexagonal platelets with deep circular pits between clusters of platelets and which had a preferred (102) orientation. Treatment of the electrolyte with activated carbon reduced the platelet size and eliminated the pits; the orientation remained (102) preferred. The orientation data for the purified electrolyte are summarized in Table 7.

The high concentrations of either D2EHPA or Alamine 336 ( $25 \text{ mg l}^{-1}$ ) or their combined presence ( $10 \text{ mg l}^{-1}$  each) in the electrolyte had only a slight effect on the zinc deposits, resulting in edge burn when the electrolyte was not treated with activated carbon. Treatment of these electrolytes with activated carbon removed the edge burn in

the case of D2EHPA and the D2EHPA–Alamine 336 combination while activated carbon and chloride ion eliminated edge burn in the case of Alamine 336. In most cases the preferred deposit orientation was (102) (114), Table 7.

The high concentrations of Kelex 100 and Versatic 911 or TBP, on the other hand, had a strong effect on the zinc deposits, resulting in severe organic burn which produced powdery and dendritic deposits. Although smooth deposits were obtained after treatment of these electrolytes with activated carbon, the deposit edges still showed signs of organic burn, and in the case of TBP, the deposit surface was dark grey. Further, the (002) deposit orientation, which resulted from the activated carbon treatment, indicated that some impurity remained active in the electrolyte. It is interesting to note that the combined effects of activated carbon and chloride ion restored the characteristic (112) orientation although the deposit edge burn and grey colour still persisted, Table 7.

Table 7. Effect of various organic extractants and  $Cl^-$  concentration on the orientation of zinc deposits obtained from activated carbon treated and untreated acid sulphate electrolytes. Electrolysis conditions:  $55\text{ g l}^{-1}\text{ Zn}$ ,  $150\text{ g l}^{-1}\text{ H}_2\text{SO}_4$ ,  $807\text{ A m}^{-2}$ ,  $35^\circ\text{ C}$

Kelex 100 ( $\text{mg l}^{-1}$ )	Versatic 911 ( $\text{mg l}^{-1}$ )	D2EHPA ( $\text{mg l}^{-1}$ )	TBP ( $\text{mg l}^{-1}$ )	Alamine 336 ( $\text{mg l}^{-1}$ )	$Cl^-$ ( $\text{mg l}^{-1}$ )	Electrolyte treated	Deposit remarks	Orientation*	Corresponding figure in text
0	0	0	0	0	0	yes	crystalline	(112)	5a
10	300	0	0	0	0	no	powder†	—	5b
10	300	0	0	0	0	yes	slight edge burn	(002)	5c
10	300	0	0	0	500	yes	edge burn	(112)	—
0	0	25	0	0	0	no	edge burn	(114) (102)	5d
0	0	25	0	0	0	yes	crystalline	(102) (103)	5e
0	0	25	0	0	100	yes	crystalline	(114) (102)	—
0	0	0	25	0	0	no	powder‡	—	—
0	0	0	25	0	0	yes	dark grey; smooth	(002)	—
0	0	0	25	0	100	no	dark grey	(112) (114)	5f
0	0	0	0	25	0	no	edge burn	(102) (114)	—
0	0	0	0	25	0	yes	edge burn	(102) (114)	—
0	0	0	0	25	100	yes	crystalline	(102) (114)	—
0	0	10	0	10	0	no	top burn	(102)	—
0	0	10	0	10	0	yes	crystalline	(102)	—
0	0	10	0	10	100	yes	crystalline	(102) (114)	—

\* Relative to ASTM standard for zinc powder.

† Deposit not suitable for XRD.

‡ Deposit not suitable for XRD or SEM.

Table 8. Effect of organic extractants on the orientation of zinc deposits obtained from industrial acid sulphate electrolyte. Electrolysis conditions: 55 g l<sup>-1</sup> Zn, 150 g l<sup>-1</sup> H<sub>2</sub>SO<sub>4</sub>, 807 A m<sup>-2</sup>, 35° C

Kelex 100 (mg l <sup>-1</sup> )	Versatic 911 (mg l <sup>-1</sup> )	D2EHPA (mg l <sup>-1</sup> )	TBP (mg l <sup>-1</sup> )	Alamine 336 (mg l <sup>-1</sup> )	Deposit remarks	Orientation*	Corresponding figure in text
5	0	0	0	0	crystalline	(1 1 2)	—
10	0	0	0	0	crystalline	(1 0 2)	—
25	0	0	0	0	organic burn	(1 0 0) (1 1 0)	6
50	0	0	0	0	organic burn	(1 1 0)	—
0	50	0	0	0	powder surface	(1 0 1)	—
0	0	5	0	0	crystalline	(1 0 1)	—
0	0	10	0	0	crystalline	(1 0 1)	—
0	0	25	0	0	organic burn	(1 0 0) (1 1 0)	—
0	0	0	5	0	crystalline	(1 0 1)	—
0	0	0	10	0	organic burn	(1 0 1)	—
0	0	0	0	6	crystalline	(1 0 1) (1 0 2)	—
0	0	0	0	9	crystalline	(1 0 1) (1 0 2)	—
0	0	0	0	30	organic burn	(1 0 1) (1 0 2)	—

\* Relative to ASTM standard for zinc powder.

### 3.4. The effect of organic extractants on zinc deposit structures obtained from industrial acid sulphate electrolyte

The effect of various organic extractants on the morphology and orientation of 1 h zinc deposits obtained from industrial acid sulphate electrolyte was briefly examined. The electrolyte had the following average analysis: Zn 150 mg l<sup>-1</sup>, MgSO<sub>4</sub> 38 mg l<sup>-1</sup>, Mn 1.6 mg l<sup>-1</sup>, Cd 0.3 mg l<sup>-1</sup>, Sb 0.02 mg l<sup>-1</sup>, Co 0.3 mg l<sup>-1</sup>, Ge 0.01 mg l<sup>-1</sup>, Ni 0.1 mg l<sup>-1</sup>, Cu 0.1 mg l<sup>-1</sup>, Fe 0.9 mg l<sup>-1</sup>, Pb 0.2 mg l<sup>-1</sup>, Cl<sup>-</sup> 80 mg l<sup>-1</sup>, Fe 3 mg l<sup>-1</sup>. Compared to the synthetic electrolyte, the deposit tolerance limit for these impurities was increased in the industrial electrolyte. The results are summarized in Table 8 which indicates the effect of various concentrations of organic extractants on the nature and orientation of the deposit.

The deposit did not exhibit evidence of organic burn until the Kelex 100 concentration was 25 mg l<sup>-1</sup>; even at 50 mg l<sup>-1</sup> Kelex 100, severe organic burn was confined to the top and edges of the deposit such that it was suitable for XRD and SEM examination. These high Kelex 100 concentrations resulted in zinc deposits having a 'clamshell' type morphology as shown in the SEM photomicrograph, Fig. 6; the preferred orientations for deposits obtained under these conditions were (1 0 0) (1 1 0), Table 8. A similar zinc deposit

morphology and orientation were reported by Robinson and O'Keefe [12] for industrial electrolyte containing high glue concentrations.

As was the case for the synthetic zinc sulphate electrolyte, additions of D2EHPA to 10 mg l<sup>-1</sup> to the industrial electrolyte resulted in a deposit structure consisting of large, well-defined hexagonal platelets aligned at intermediate angles to the aluminium cathode; the preferred orientation was (1 0 1). Increasing the concentration of D2EHPA in the electrolyte to 25 mg l<sup>-1</sup> resulted in a 'clamshell' type deposit morphology; the deposit orientation was (1 0 0) (1 1 0) and organic burn occurred at the edges.

Organic burn was observed for TBP concentrations of 10 mg l<sup>-1</sup> in the electrolyte; the deposit orientation was (1 0 1). An Alamine 336 concentration of 30 mg l<sup>-1</sup> was required before organic burn was evident. The presence of Alamine 336 in the electrolyte gave a deposit which consisted of large hexagonal platelets having a (1 0 1) (1 0 2) preferred orientation.

The increased tolerance of the industrial electrolyte to the various organic extractants may be attributed to the high level of MgSO<sub>4</sub> and gypsum in the electrolyte. As a result, the industrial electrolyte is more viscous than the synthetic electrolyte so that the diffusion of the organic species to the cathode surface is likely to be slower in the industrial electrolyte.

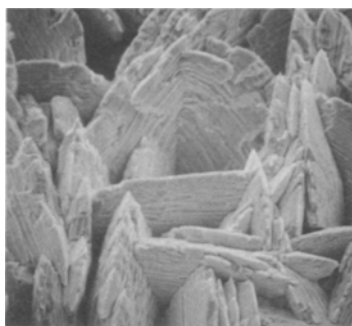


Fig. 6. SEM photomicrograph showing the effect of Kelex 100 ( $25 \text{ mg l}^{-1}$ ) on the morphology of a zinc deposit obtained from industrial electrolyte.  $807 \text{ A m}^{-2}$ , ( $\times 840$ ).

Some preliminary tests in which  $10 \text{ mg l}^{-1}$  Kelex 100 was added to a synthetic electrolyte doped with  $38 \text{ g l}^{-1} \text{ MgSO}_4$  resulted in a zinc deposit having a (100) preferred orientation and a 'clamshell' type morphology, similar to that obtained for the addition of Kelex 100 to the industrial electrolyte (Fig. 6).

### 3.5. The effect of chloride ion and organic extractants on zinc deposition polarization

The effects of chloride ion and organic extractants on zinc deposition polarization in synthetic electrolyte were studied in order to determine if a correlation between deposit morphology and zinc

deposition overvoltage could be established. Fig. 7 shows a series of potentiodynamic current-potential curves for zinc deposition. The polarization curve was unaffected by  $\text{Cl}^-$  concentration up to  $500 \text{ mg l}^{-1}$ ; identical curves were obtained from both addition-free electrolyte and electrolyte containing  $500 \text{ mg l}^{-1} \text{ Cl}^-$ , Fig. 7. This is in accord with the fact that  $\text{Cl}^-$  concentrations to  $500 \text{ mg l}^{-1}$  had no substantial effect on the morphology and orientation of zinc deposits obtained at  $269 \text{ A m}^{-2}$  and that  $\text{Cl}^-$  had only a slight effect at the  $500 \text{ mg l}^{-1}$  level for deposits obtained at  $807 \text{ A m}^{-2}$ .

The results presented earlier indicated that the zinc deposit morphology and orientation showed a reasonable tolerance to the presence of D2EHPA and Alamine 336 in the electrolyte. Zinc deposition polarization curves obtained from electrolyte containing  $25 \text{ mg l}^{-1}$  of these extractants indicate that both D2EHPA and Alamine 336 cause only a small increase in the polarization as compared to the addition-free curve, Fig. 7.

The most striking effect was obtained when the electrolyte contained  $10 \text{ mg l}^{-1}$  Kelex 100 or  $10 \text{ mg l}^{-1}$  TBP in which case the zinc deposition reaction became strongly polarized (Fig. 7). Again, this finding is in good agreement with the effects of these extractants on the zinc deposit characteristics described earlier. Kelex 100, in particular,

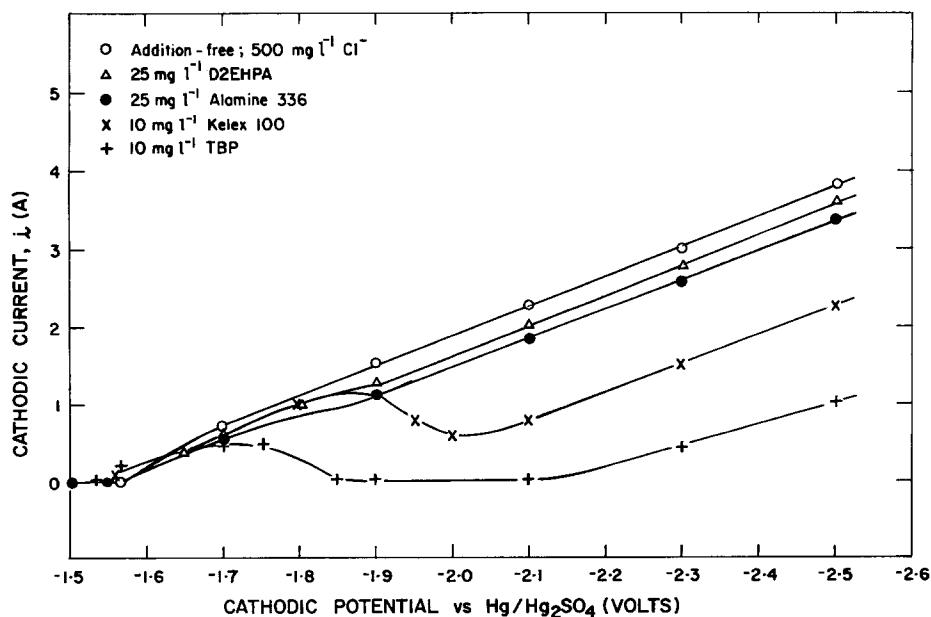


Fig. 7. Current-potential plots showing the effect of  $\text{Cl}^-$  and organic extractants on zinc deposition polarization.

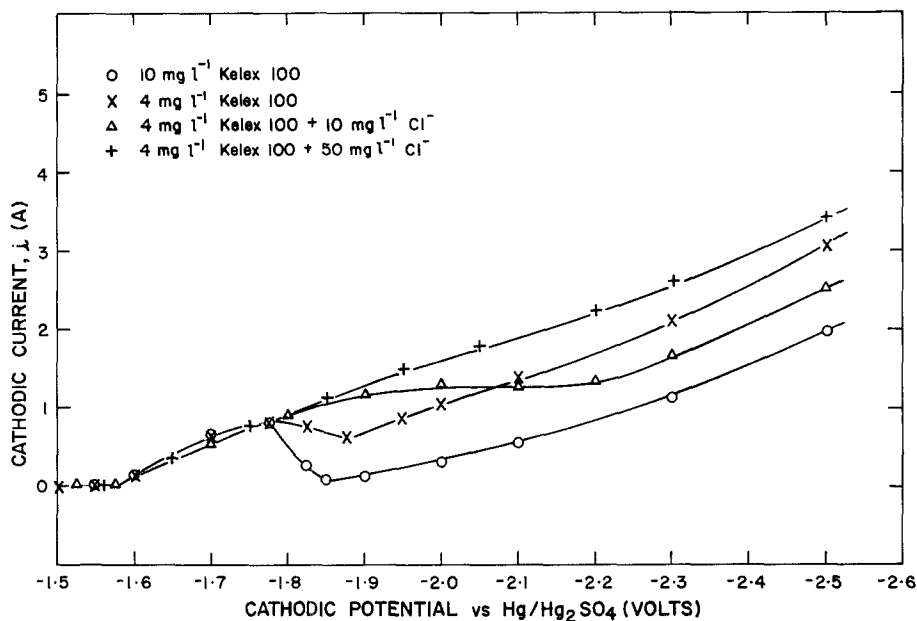


Fig. 8. Current-potential plots showing the effect of Kelex 100 and Kelex 100 + Cl<sup>-</sup> on zinc deposition polarization.

was observed to cause severe organic burn to the deposit when present in the electrolyte at concentration  $> 2 \text{ mg l}^{-1}$ . Furthermore, when present in the industrial electrolyte which showed a strong tolerance to these extractants in terms of deposit quality, these extractants changed the deposit orientation to strongly preferred (110)(100) which resulted in an unusual 'clamshell' type morphology.

In Fig. 8, the effect of Kelex 100 on zinc deposition polarization is examined in more detail. The polarization effect is less severe when the Kelex 100 concentration is reduced to 4 ppm; more significantly, the polarization is completely removed when  $\text{Cl}^- > 50 \text{ mg l}^{-1}$  is present in the electrolyte. This suggests that the presence of sufficient  $\text{Cl}^-$  in the electrolyte counteracts the polarizing effect of Kelex and confirms the results obtained from SEM and OM presented earlier.

#### 4. Conclusions

The effects of chloride ion and organic extractants alone and in various combinations (such as those which could be present in zinc sulphate electrolyte produced by solvent extraction) on the structure of zinc deposits obtained under a variety of experimental conditions have been examined. Chloride

ion was found to have a significant effect on the deposit morphology and orientation only when its concentration in the electrolyte reached  $500 \text{ mg l}^{-1}$  and when the cathodic current density was greater than  $269 \text{ A m}^{-2}$  ( $25 \text{ A ft}^{-2}$ ). The zinc deposits were adversely affected by the presence of organic extractants in the electrolyte at concentrations well below their solubility limits. In some cases the adverse effects of these organic extractants were offset by the presence of sufficient  $\text{Cl}^-$  in the electrolyte. In addition, purification of electrolyte contaminated with organic extractants by treatment with activated charcoal resulted in a vastly improved deposit structure.

In general, the effects of  $\text{Cl}^-$  and organic extractants on the zinc deposit structure correlated with their effects on zinc deposition polarization curves. Thus the use of polarization techniques for monitoring zinc deposition may provide a useful means for characterizing zinc sulphate electrolyte prepared by solvent extraction processes.

#### Acknowledgements

Helpful discussions with R. C. Kerby, Cominco Ltd, throughout the course of this work are gratefully acknowledged. Thanks are due to Cominco

Ltd for supplying the electrolyte, glue and cathode aluminium and to R. Packwood, CANMET for providing the SEM facilities. J. M. Stewart and E. J. Murray, CANMET, did the X-ray diffraction measurements and Y. Bourgoin, CANMET, prepared the polished sections for optical microscopy. One of us (V. I. L.) gratefully acknowledges the National Research Council, Canada for awarding a fellowship.

## References

- [1] D. M. Muir, D. C. Gale, A. J. Parker and D. E. Giles, *Proc. Australas. Inst. Min. Metall.* **259** (1975) 23.
- [2] F. P. Haver, D. L. Bixby and M. M. Wong, U.S. Bureau of Mines Report of Investigations RI 8276 (1978) p. 11.
- [3] J. E. Dutrizac and R. J. C. MacDonald, *Minerals Sci. Engng.* **6** (1974) 59.
- [4] H. W. Parsons and G. M. Ritcey, *Northern Miner* **63** (37) (1977) D-20.
- [5] N. M. Rice and M. R. Smith, *Canad. Met. Quart.* **12**(3) (1973) 341.
- [6] V. I. Lakshmanan and G. J. Lawson, *Proc. Int. Solvent Extraction Conf.* Vol. II (1974) 1169.
- [7] A. K. Haines, T. H. Tunley, W. A. M. Te Riele, F. L. D. Cloete and T. D. Sampson, *J. South Afr. Inst. Min. Metall.* Nov. (1973) 149.
- [8] J. M. R. Vega and E. D. Nogueira, US Patent no. 3 (1975) 923, 976.
- [9] H. Fukubayashi, T. J. O'Keefe and W. C. Clinton, U.S.B.M. Report of Investigations, RI 7966 (1974) p. 26.
- [10] D. R. Fosnacht and T. J. O'Keefe, *the Poster Session, AIME Meeting*, Atlanta (1977).
- [11] R. C. Kerby, H. E. Jackson, T. J. O'Keefe and Yar-Ming Wang, *Metall. Trans.* **8B** (1977) 661.
- [12] D. J. Robinson and T. J. O'Keefe, *J. Appl. Electrochem.* **6** (1976) 1.
- [13] D. J. MacKinnon, J. M. Brannen and R. C. Kerby, *ibid* **9** (1979) 55.
- [14] D. J. MacKinnon and J. M. Brannen, *ibid* **7** (1977) 451.
- [15] R. Brugger 'Nickel Plating', Robert Draper Ltd, Teddington, England (1970) Ch. 13, p. 258.